Archives of Medical Reports

2(6) (2025) 13-24

OPEN ACCESS

RESEARCH ARTICLE

A Multimodal Approach of Beta-Sitosterol-Coated Zinc Oxide Nanoparticles for Combating Oral Pathogens and Oral Cancer

Sakshi Saxena[1,*], Sadhana Kumaran[2]

[1] Peoples Dental Academy, Peoples Campus, Bhanpur, Bhopal-462037, Madhya Pradesh, India

[2] Department of Chemistry, Government Thirumagal Mill's College, Gudiyatham – 632602, Tamil Nadu, India

***Corresponding Author:** Sakshi Saxena
Peoples Dental Academy, Peoples Campus, Bhanpur, Bhopal-462037, Madhya Pradesh, India.
Email: drsakshi2111@gmail.com

Articleinfo
Received: 20 September 2025
Accepted: 25 November 2025

Keywords: Oral pathogens, Oral Cancer, Antibiotic Resistance, Zinc Oxide Nanoparticles, Beta Sitosterol.

How to cite this article: Sakshi Saxena. (2025). A Multimodal Approach of Beta-Sitosterol-Coated Zinc Oxide Nanoparticles for Combating Oral Pathogens and Oral Cancer, 2(6), 13-24 Retrieved from https://archmedrep.com/index.php/amr/article/view/72

Abstract

Oral health problems such as infections, tooth decay, and gum disease, often caused by oral pathogens, are increasingly linked to oral cancer. This study successfully synthesized and characterized beta sitosterol functionalized ZnO nanoparticles (BS-ZnO NPs), with UV-Visspectroscopy showing a prominent absorption peak at 302 nm, and FTIR analysis confirming the functionalization through characteristic peaks of O–H, C=C, C–O, and Zn–O bonds. SEM and XRD analyses revealed their crystalline nature and morphology. The antioxidant potential of BS-ZnO NPs, demonstrated through DPPH and ABTS assays, showed a dose-dependent radical scavenging activity comparable to standard antioxidants. Antimicrobial activity against *Streptococcus aureus, Enterococcus faecalis, Candida albicans*, and *Staphylococcus mutans* revealed significant growth inhibition and superior efficacy to amoxicillin at equivalent concentrations. Molecular docking studies highlighted strong binding affinities of BS with pathogen virulence proteins, including Als3 adhesin in *C. albicans* and *phospholipase C* in *S. aureus*, disrupting biofilm formation and microbial adhesion. Additionally, BS-ZnO NPs exhibited potent anticancer activity against KB oral cancer cells, reducing cell viability to 28% at 100 µg/mL and outperforming cyclophosphamide. Gene expression analysis showed significant downregulation of the anti-apoptotic gene Bcl-2 and upregulation of pro-apoptotic Bax and tumor suppressor p53, highlighting their role in modulating apoptotic pathways. These findings underscore the multifunctional potential of BS-ZnO NPs as promising agents for oral health applications, including antioxidants, antimicrobials, and targeted therapeutics for oral cancer.

1. Introduction

Oral health problems, including oral infections and oral cancer, represent significant challenges to global health. Oral pathogens such as *Streptococcus mutans, Enterococcus faecalis, Staphylococcus aureus,* and *Candida albicans* contribute a vital role in the pathological process of oral disorders (Amaya Arbeláez et al., 2021; Li et al., 2022). These microorganisms create a conducive environment for microbial proliferation and inflammation, often leading to tooth decay, gum disease, and systemic complications. Dental caries can progress from enamel demineralization to deeper infections affecting the dental pulp, potentially resulting in abscess formation and severe pain (Roberts et al., 2022). Chronic periodontal diseases, such as periodontitis and gingivitis, cause progressive destruction of the supporting tissues around the teeth, eventually leading to tooth loss (Junge et al., 2021). Beyond these localized effects, oral infections are increasingly associated with systemic health issues, including the development of oral cancer. Chronic inflammation induced by periodontal pathogens is believed to foster conditions conducive to carcinogenesis (Li et al., 2022). Oral squamous cell carcinoma (OSCC), the most common form of oral cancer, remains challenging to manage due to its rapid progression and frequent late-stage diagnosis (Ravikumar et al., 2024). Current treatment options, including immunotherapy, chemotherapy, targeted therapy, radiation therapy, and

surgery are often possess significant side effects and variable outcomes. Furthermore, rising antibiotic resistance among oral pathogens underscores the urgent need for innovative therapeutic strategies to combat both oral infections and cancer effectively.

Nanotechnology offers promising solutions to these challenges by enabling the development of multifunctional therapeutic agents. Zinc oxide nanoparticles (ZnO NPs) have attracted interest due to their impressive characteristics, such as a large surface area relative to their volume, compatibility with biological systems, and strong antimicrobial and anticancer effects (Tayyeb et al. 2024). ZnO NPs can induce apoptosis in cancer cells, suppress proliferation, and modulate signalling pathways critical for cell survival (Shaik et al., 2024). Their antibacterial properties are effective against a wide range of pathogens, including strains resistant to drugs, which positions them as a valuable resource in overcoming the challenges posed by traditional treatments. Beta-sitosterol (BS), a natural plant compound, has strong therapeutic potential due to its antioxidant, anti-inflammatory, and anticancer effects. It helps regulate cholesterol levels, boosts the immune system, and can trigger cell death and slow tumor growth through various molecular pathways (Khan et al., 2022). The combination of beta-sitosterol and ZnO NPs presents an innovative strategy to maximize their synergistic effects. BS-ZnO NPs offer a dual therapeutic approach by enhancing antibacterial activity against resistant pathogens while exhibiting anticancer properties through the regulation of apoptotic pathways. This study focuses on the synthesis and characterization of BS-ZnO NPs using advanced analytical techniques. The antibacterial, antioxidant, and anticancer effects of these NPs were evaluated to explore their potential in addressing the dual challenges of oral infections and oral cancer.

2. Materials and Methods

2.1. BS-ZnO NPs synthesis

The synthesis of beta-sitosterol-functionalized zinc oxide nanoparticles (BS-ZnO NPs) was initiated by preparing a 10 mg/mL BS solution through the dissolution of 50 mg of beta-sitosterol in 5 mL of ethanol. Concurrently, 20 mL of 0.1 M zinc acetate dihydrate solution was prepared and stirred continuously at room temperature. The BS solution was then gradually introduced into the zinc acetate solution under constant stirring. The pH of the mixture was adjusted to approximately 10 by the dropwise addition of 0.1 M sodium hydroxide solution. To ensure the reaction's completion, the mixture was stirred for an additional two hours. The resulting nanoparticles were collected via centrifugation at 8000 rpm for 10 minutes, washed with distilled water to remove residual impurities, and subsequently vacuum-dried at 60°C for 12 hours. Characterization of the synthesized BS-ZnO NPs was performed using UV-Vis spectroscopy to determine their optical bandgap energy, scanning electron microscopy (SEM) to evaluate morphology and size distribution, X-ray diffraction (XRD) to analyze crystallographic phases and crystalline size, and Fourier-transform infrared spectroscopy (FTIR) to identify functional groups and confirm chemical composition(Tayyeb et al., 2024a).

2.2. Antioxidant assay

The antioxidant potential of BS-ZnO NPs was assessed using the 2,2-diphenyl-1-picrylhydrazyl (DPPH) assay. A 0.1 mM DPPH solution was prepared in ethanol, and varying concentrations of BS-ZnO NPs (5, 25, 50, and 100 µg/mL) were prepared. For each concentration, 100 µL of the nanoparticle solution was mixed with 900 µL of the DPPH solution. The mixtures were incubated in the dark at room temperature for 30 minutes to allow for the reaction. Following incubation, the absorbance of each mixture was measured at 517 nm using a UV-Vis spectrophotometer to determine the DPPH radical scavenging activity of the BS-ZnO NPs (Hussain et al., 2024).

The antioxidant activity of BS-ZnO NPs was evaluated using the 2,2′-azino-bis-(3-ethylbenzothiazoline-6-sulfonic acid) (ABTS) assay, which measures the scavenging of ABTS•+ radicals. ABTS solution (7 mM) and potassium persulfate (2.45 mM) were mixed and allowed to react in the dark at room temperature for 16 hours to generate ABTS+ radical cations. The resultant solution was diluted with ethanol to achieve an absorbance of 0.70 ± 0.02 at 734 nm. To assess antioxidant activity, BS-ZnO NPs were prepared at concentrations of 5, 25, 50, and 100 µg/mL. A volume of 900 µL of the diluted ABTS+ solution was mixed with 100 µL of BS-ZnO NPs at each concentration. The mixtures were incubated in the dark at room temperature for six months. Absorbance was measured at 734 nm using a UV-Vis spectrophotometer to determine the radical scavenging activity of BS-ZnO NPs (Rafe Hatshan et al., 2024).

2.3. Antimicrobial assay

The microdilution method determined the minimum inhibitory concentration (MIC) of BS-ZnO NPs against oral pathogens, including *S. mutans, S. aureus, E. faecalis,* and *C. albicans*. In a sterile 96-well microtiter plate, 100 µL of serially diluted BS-ZnO NPs solutions were added to wells, followed by 100 µL of a pathogen suspension (~1.5×10^5 CFU/mL). The plate was incubated at 37°C for 24 hours. Finally, turbidity for each well was measured at 590 nm (Ahmad et al., 2021).

The inhibitory zone activity of BS-ZnO NPs against oral pathogens was assessed using the well diffusion method. Using sterile cotton swabs, the bacterial suspension was evenly spread over Basal medium agar plates were

inoculated with a standardized microbial suspension evenly spread with a sterile swab. Wells were created in the agar using a sterile cork borer, and 20 µL of BS-ZnO NPs were dispensed into each well. Positive control wells containing a standard antibacterial agent were included. The plates were incubated for 24 hours and the diameter of the zone of inhibition was measured (Alam et al., 2021).

2.4. Ligand-receptor interaction studies

Molecular docking of BS with receptors of oral pathogens was performed using AutoDock. The 3D structure of BS was sourced from the PubChem database. Structures of the receptors were obtained from the PDB. Preparation of ligands and receptors in AutoDock Tool 1.5.7 included the addition of hydrogens, charges, and essential bonds. Active site residues were identified, and grid box parameters were established for the docking procedure. Docking was executed using the Lamarckian genetic algorithm, and molecular interactions were illustrated using Discovery Studio Visualizer (Kandaswamy et al., 2024).

2.5. Apoptosis assay

The anti-cancer activity of BS-ZnO NP was determined using the Hela tumor cell line (KB cells). Briefly, the cells were obtained from the National Centre for Cell Repository (NCCS) and were maintained in a DMEM medium supplemented with 10% FBS and 0.05% penicillin-streptomicin solution at 37°C with 5% CO_2. For the MTT assay, the cells were seeded into 96 well plates, in which each well contained ~1×10^4 cells. The cells were exposed to different concentrations of BS-ZnO NPs for a duration of 24 hours. After exposure, the solutions were removed and the cells were rinsed thrice with Phosphate buffer and treated with MTT solution (5 mg/mL in PBS) for 4 hours in dark at 37°C. The formazan crystals formed were dissolved into DMSO and absorbance was recorded at 579 nm (Marunganathan et al., 2024).

2.6. Apoptosis gene expression

The total RNA was obtained from KB cells that were treated with BS-ZnO NPs using the Trizol reagent. After extracting RNA, the sample was purified with ethanol, precipitated using isopropanol, and then resuspended in TE buffer. The purity of the RNA extracted was determined using a NanoDrop spectrophotometer. From RNA, cDNA was generated using a reverse transcription kit, with the RNA incubating at 37°C. The reaction was halted by heating to 95°C for five minutes, and the cDNA was preserved for subsequent analysis. The cDNA were then taken for qRT-PCR analysis. qRT-PCR was performed with conditions including 40 cycles of denaturation at 95°C for thirty seconds (Table 1). Gene expression was analyzed using the $2^{-\Delta\Delta Ct}$ method, with normalization to GAPDH (Livak and Schmittgen, 2001).

Table 1. List of Primer sequence used for gene expression

Gene	Forward primer (5´-3´)	Reverse primer (5´-3´)	Reference
GAPDH	GCCAAAAGGGTCATCATCTCTGC	GGTCACGAGTCCTTCCACGATAC	(Heidari and Doosti, 2023)
BCL-2	GACGACTTCTCCCGCCGCTAC	CGGTTCAGGTACTCAGTCATCCAC	(Heidari and Doosti, 2023)
BAX	AGGTCTTTTTCCGAGTGGCAG	GCGTCCCAAAGTAGGAGAGGAG	(Heidari and Doosti, 2023)
P53	ACATGACGGAGGTTGTGAGG	TGTGATGATGGTGAGGATGG	(Hong et al., 2021)

2.7. Statistical analysis

Each experiment was repeated for three individual times and the values obtained from three independent experiment were plotted as mean ± standard deviation using GraphPad Prism 9.0. The graphs were analysed using One-way or Two-way ANOVA analysis and the all groups were compared with control using Dunnett's and Bonferroni's multiple comparison test, respectively. $p< 0.05$ was considered as significant.

3. Results

3.1. Characteristics of BS-ZnO NP

The results from UV-spectrum analysis revealed a single absorption peak at 302 nm, indicating the successful synthesis of ZnO NPs (Figure 1). The FTIR spectrum further supports the successful functionalization of ZnO NPs with BS. The broad peak observed around 3456 cm^{-1} corresponds to O–H stretching vibrations, indicating the presence of hydroxyl groups from beta-sitosterol. The sharp peak at 1637 cm^{-1} is attributed to the C=C stretching vibrations, confirming the presence of the sterol ring system, while peaks at 1372 cm^{-1} and 873 cm^{-1} correspond to C–O stretching and Zn–O bond vibrations, respectively (Figure 2). These results collectively validate the successful synthesis and coating of ZnO NPs with BS. Complementary SEM and XRD analysis further confirmed the crystalline nature of the NPs, with SEM providing insights into the morphology and XRD revealing distinct diffraction peaks characteristic of ZnO's crystalline structure (Figure 3 & 4).

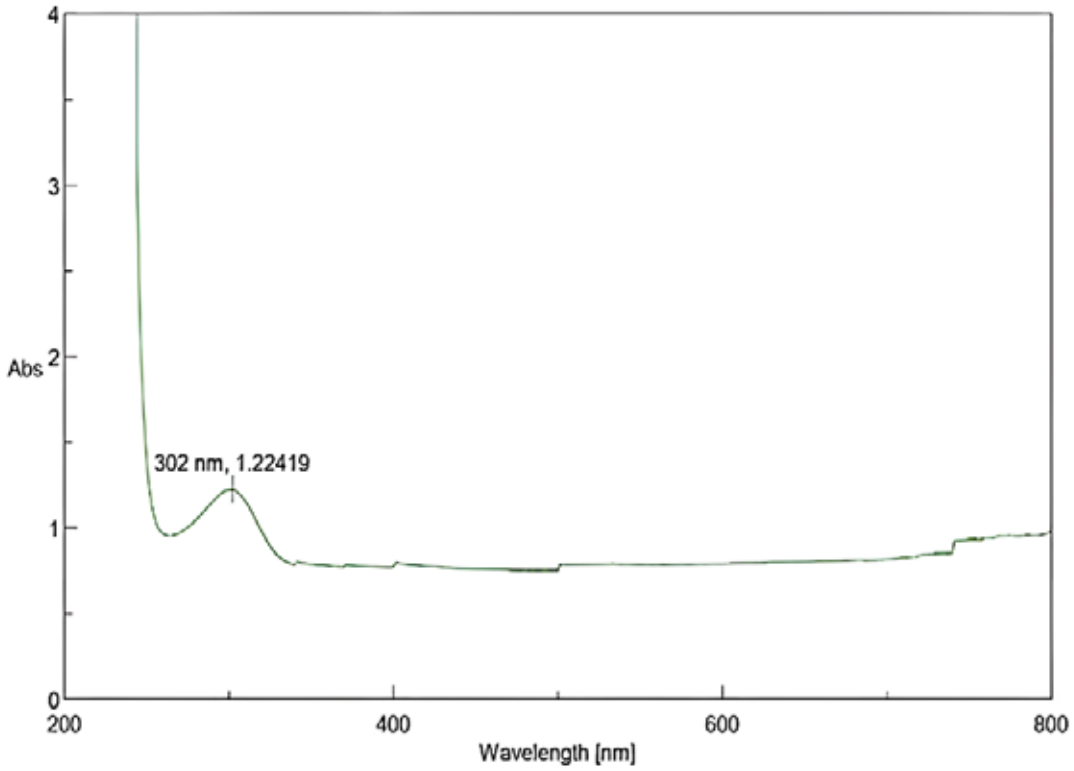

Figure 1: UV-Vis Spectral Analysis of Synthesized BS-ZnO

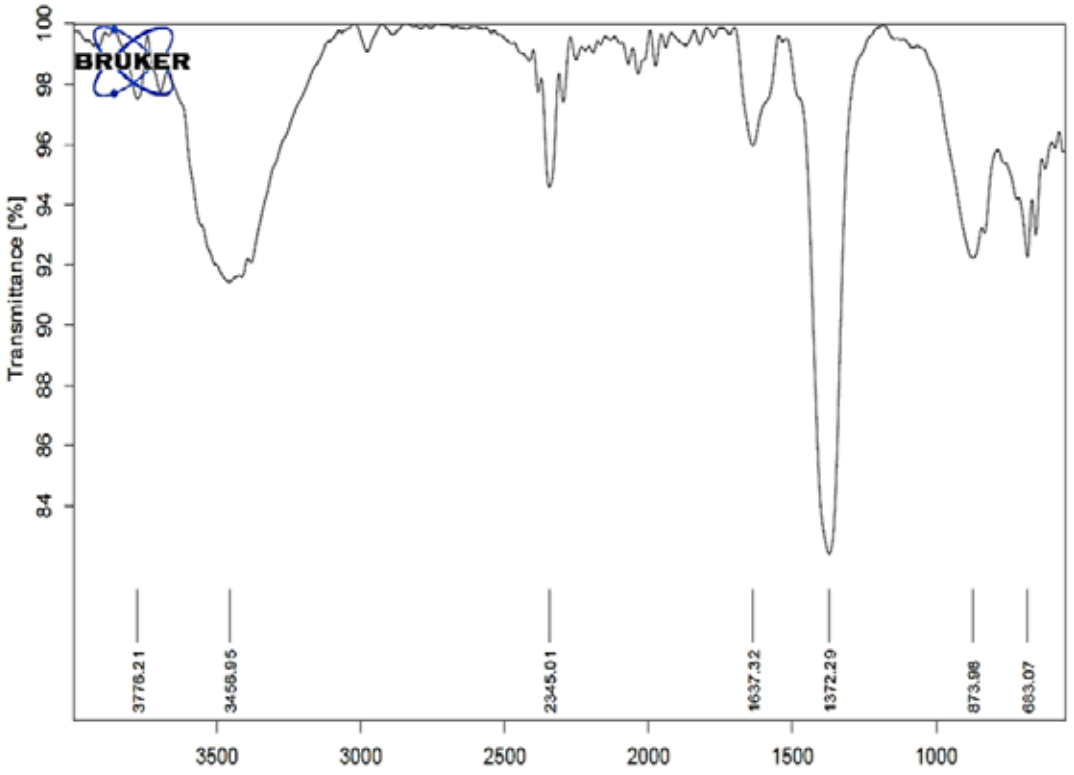

Figure 2: FTIR analysis of BS-ZnO NPs

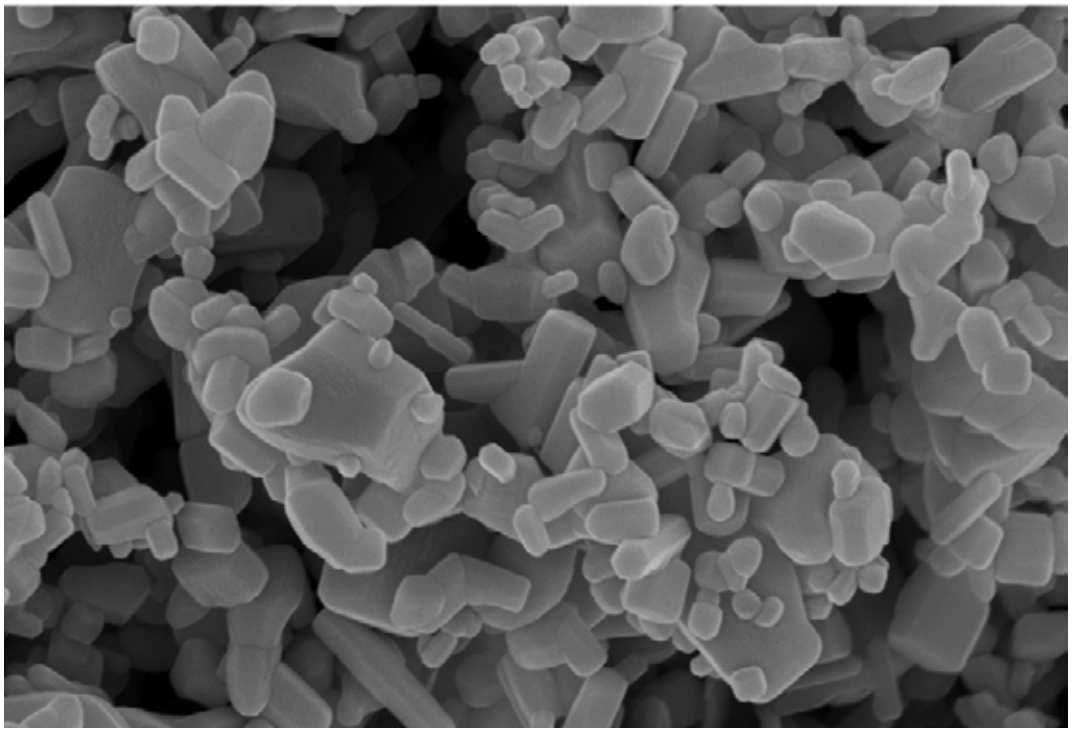

Figure 3: SEM images of BS-ZnO NPs

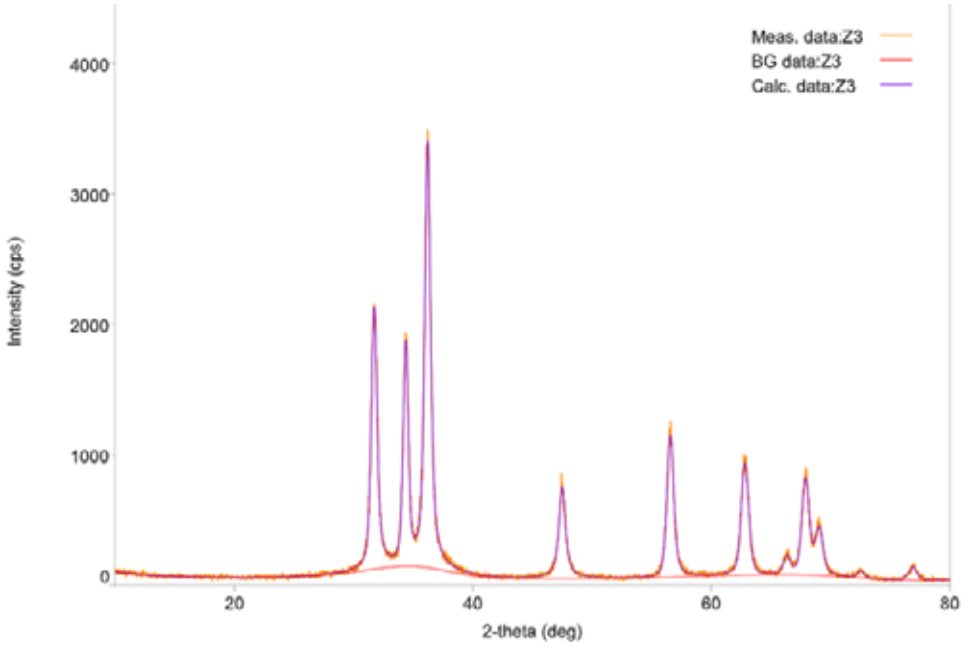

Figure 4: XRD analysis of BS-ZnO NPs

3.2. Effect of Free radical Scavenging

The free radical scavenging activity of BS-ZnO NPs was determined using the DPPH assay. Various doses of BS-ZnO NPs from 5 to 100 µg/mL were used in this experiment. At the lowest dose of 5 µg/mL, BS-ZnO NPs showed modest DPPH radical scavenging activity, with an inhibition percentage of 6%. Increasing the concentration to 100 µg/mL significantly enhanced the DPPH scavenging activity, with an inhibition percentage of 58%. This demonstrated a dose-dependent increase in antioxidant capacity (Figure 5a).

The ABTS assay demonstrated that BS-ZnO NPs exhibited strong antioxidant activity, with a clear dose-dependent increase in ABTS radical scavenging ability (Figure 5b). At a concentration of 100 µg/mL, BS-ZnO NPs showed an ABTS radical inhibition rate of 70%, which was comparable to trolox treatment at 100 µg/mL (83%).

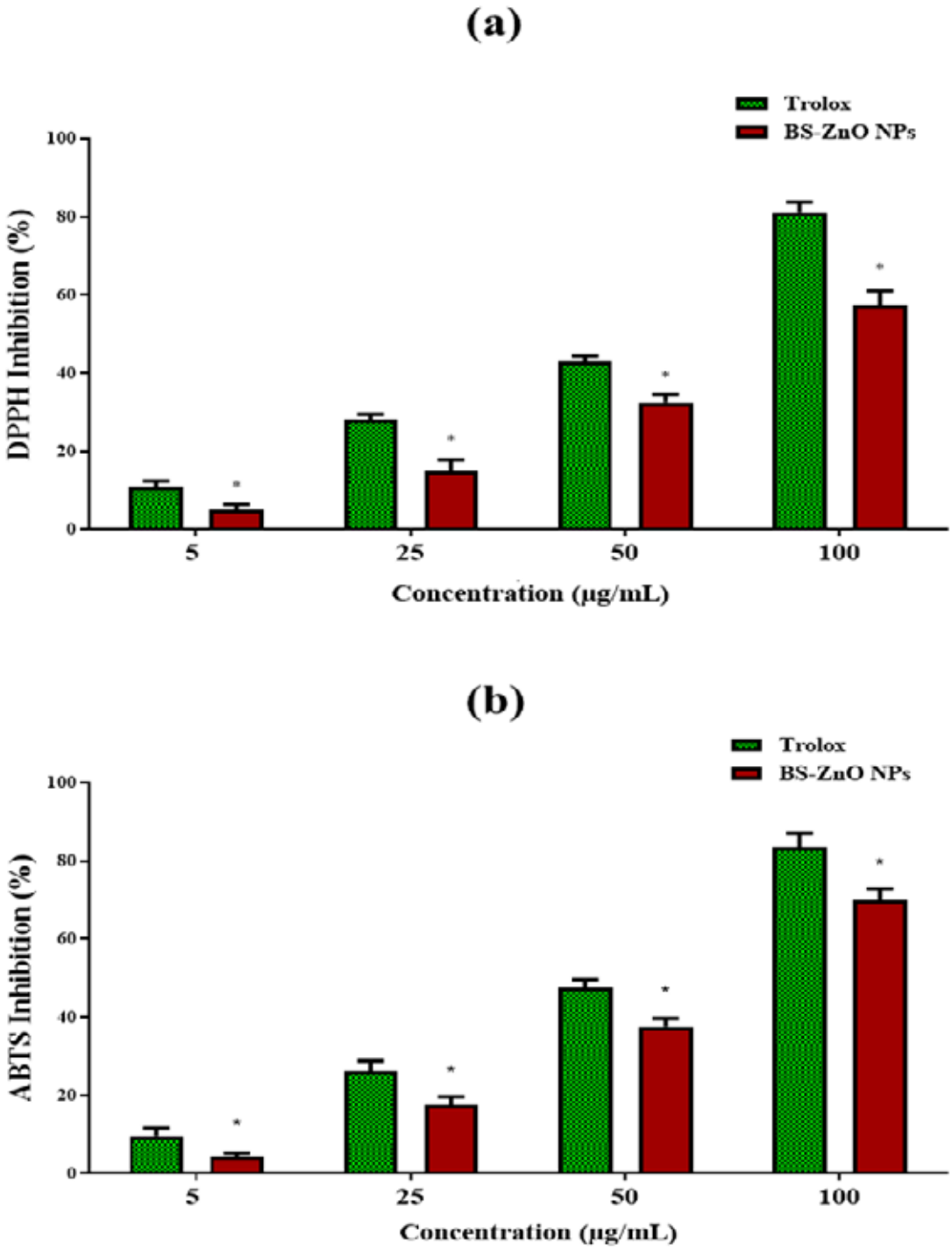

Figure 5: The radical scavenging activities of BS-ZnO NPs were evaluated using both (a) DPPH and (b) ABTS assays. Significant differences between BS-ZnO NPs and trolox were indicated by * indicated the $p < 0.05$.

3.3 BS-ZnO NPs inhibit oral pathogens

The antimicrobial activity of BS-ZnO was investigated against four oral pathogens strains. The MIC of BS-ZnO NPs was determined to be 50 µg/mL for all tested pathogens, indicating inhibition of microbial growth at this concentration (Figure 6). At a concentration of 50 µg/mL, BS-ZnO NPs produced inhibition zones of 1.1 cm for *S. aureus*, 1.0 cm for *E. faecalis*, 0.6 cm for *C. albicans*, and 0.6 cm for *S. mutans*. Whereas, at 100 µg/mL, the inhibition zones increased to 1.3 cm, 1.1 cm, 0.8 cm, and 0.9 cm, respectively (Figure 7a & b). These results suggest that BS-ZnO NPs exhibit a concentration-dependent enhancement in antimicrobial activity. BS-ZnO NPs outperformed amoxicillin in their activity against *S. aureus* and *S. mutans* at equivalent concentrations of 100 µg/mL.

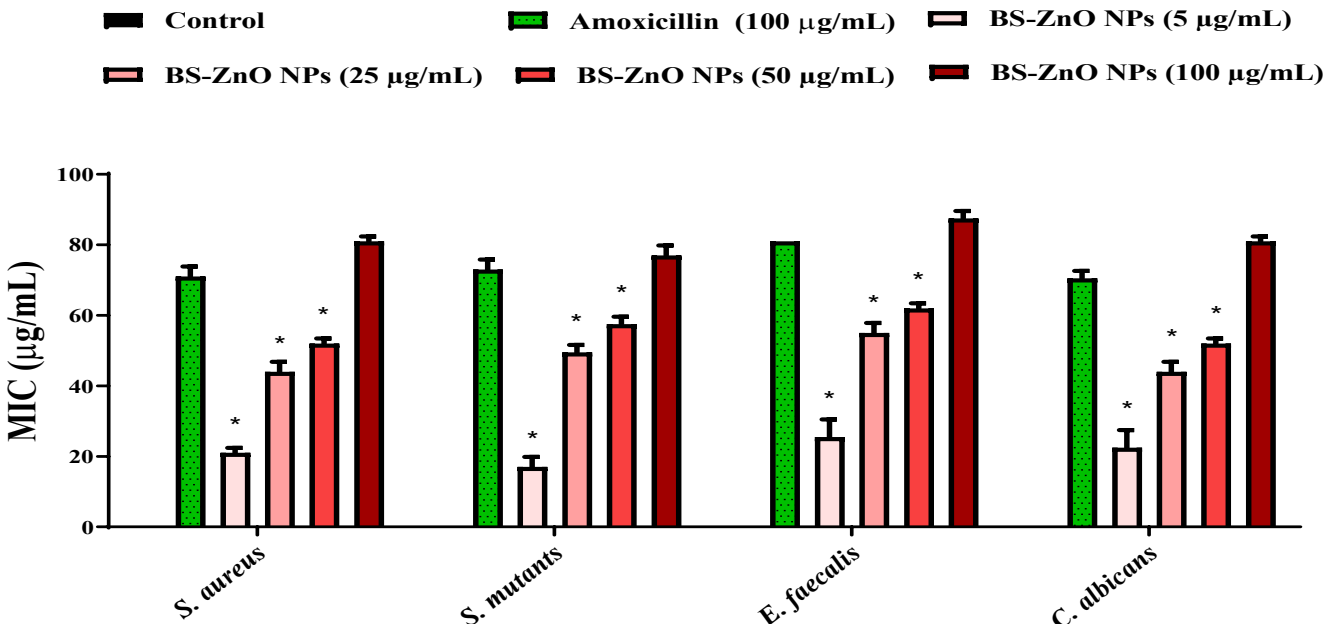

Figure 6: The MIC of BS-ZnO NPs was assessed against oral pathogens. The positive control was amoxicillin. When compared to the control, statistical significance ($p < 0.05$) is indicated by the asterisk (*).

(a)

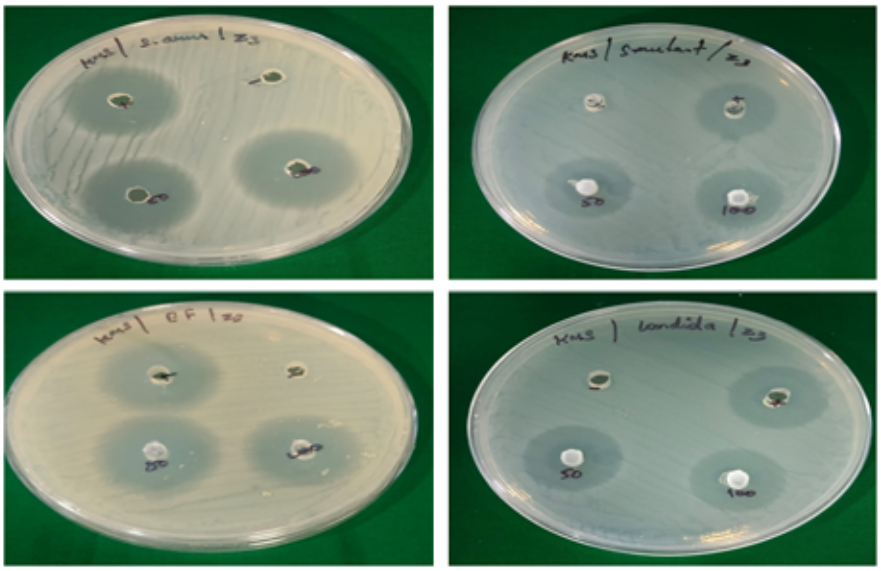

(b)

Compound	Zone of Inhibition (mm)			
	S. aureus	*E. faecalis*	*C. albicans*	*S. mutans*
Amoxicillin (100µg/ ml)	10	12	9	8
BS-ZnO NPs (50µg/ mL)	11	10	6	6
BS-ZnO NPs (100µg/ mL)	13	11	8	9

Figure 7: (a) Zone of Inhibition and (b) MIC activity of BS-ZnO NPs tested against different oral pathogens and compared with amoxicillin

3.4. BS effectively binds with microbial peptides

The molecular docking was performed between beta-sitosterol and potential anti-microbial target peptides of microbial pathogens. Among the proteins analyzed, the strongest binding affinity was observed with *C. albicans adhesin* Als3 (-6.6 kcal/mol), where BS interacted with residues such as PHE, TRP, and VAL through hydrophobic interactions and GLN through polar contacts. For *S. aureus phospholipase C* (-5.4 kcal/mol), interactions with TYR, ARG, and ILE indicate a combination of hydrophobic and electrostatic interactions. Similarly, moderate binding was observed with *S. mutans glucosyltransferase B* (-5.5 kcal/mol), where LYS, VAL, and MET residues facilitated the interaction. For *E. faecalis* enterococcal surface protein (-5.3 kcal/mol), the binding involved MET and ASN residues (Table 2 & Figure 8).

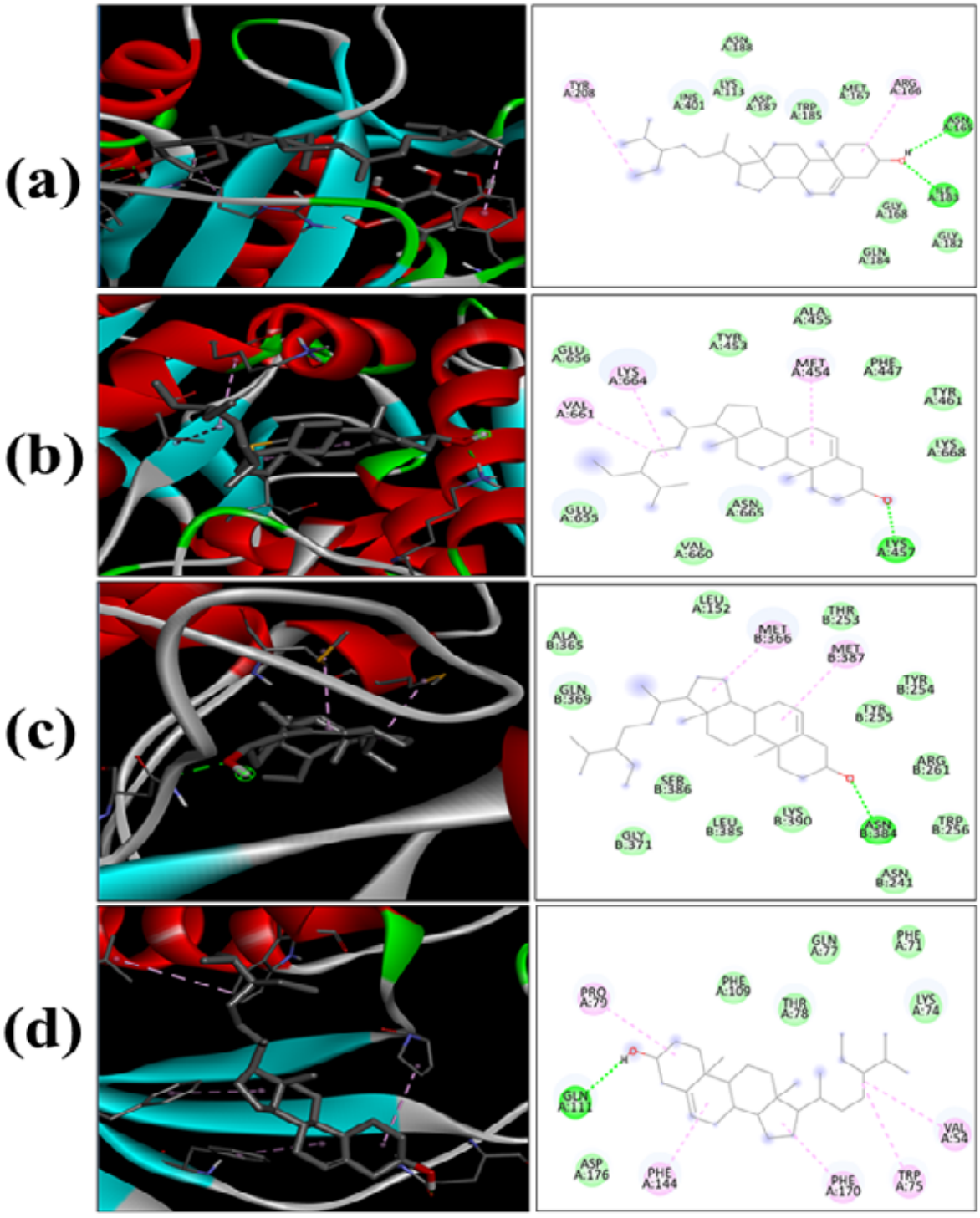

Figure 8: The interaction between oral pathogen receptors andBS are depicted includes both 2D and 3D typical representations of the interactions. (a) 3V16 of S. aureus, (b) 8FKL of S. mutans, (c) 6ORI of *E. faecalis*, (d) 4LE8 of C. albicans.

Table 2. Molecular Docking analysis of BS with different oral pathogens target proteins

Sl. No.	Protein	PDB ID	Binding affinity (kcal/mol)	Amino acids in other type of bonding except hydrogen bond
1	*S.aureus*: Phospholipase C	3V16	-5.43	TYR, ARG, ASN, ILE
2	*S. mutans*: Glucosyltransferase B	8FKL	-5.56	LYS, VAL, MET, LYS
3	*E. faecalis*: Enterococcal surface protein	6ORI	-5.39	MET, MET, ASN
4	*C. albicans*: Adhesin Als3	4LE8	-6.64	PRO. GLN, PHE, PHE, TRP, VAL

3.5. BS-ZnO NPs showed anti-cancer activity

The results from MTT assay revealed that cytotoxic effects of BS-ZnO NPs increased in dose-dependent manner. The cell viability of KB cells reduced to 28% at 100 µg/mL, which is almost similar with the activity of cyclophosphamide, which reduced cell viability to 35% at 100 µg/mL (Figure 9).

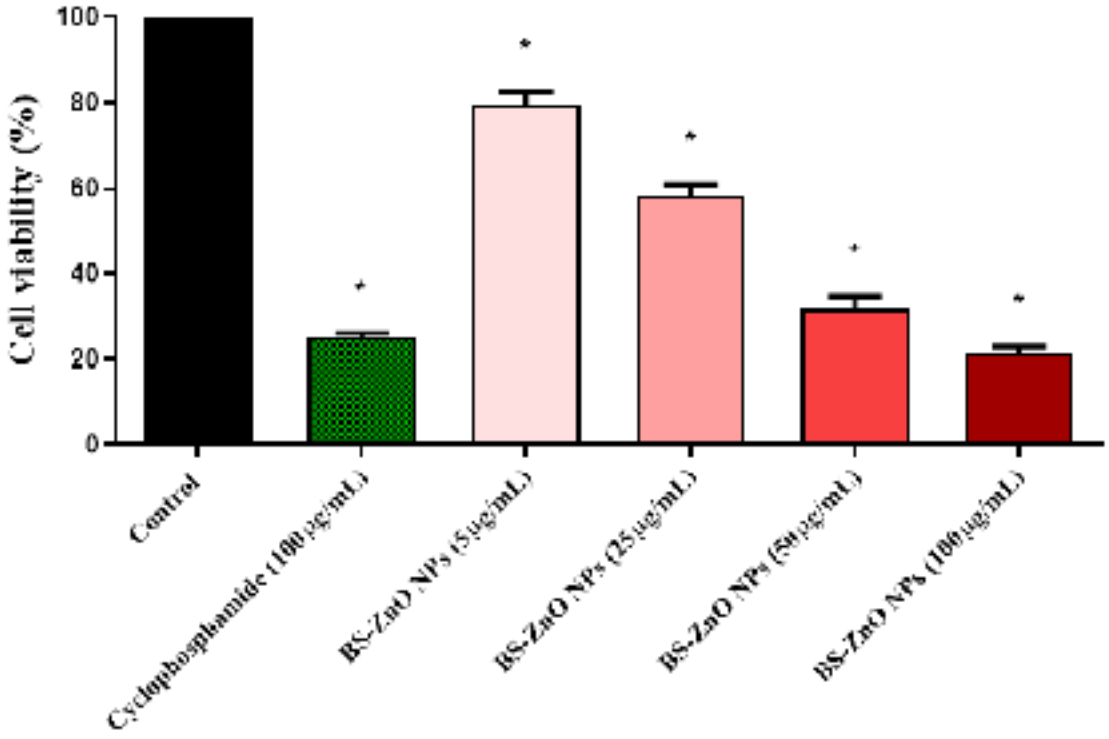

Figure 9: Cytotoxic effect of BS-ZnO NPs on KB oral cancer cells compared to cyclophosphamide.

3.6. Molecular mechanism of BS-ZnO NPs

The results from gene expression analysis revealed that expression of anti-apoptotic protein Bcl-2 (0.8-fold) was substantially downregulated by the treatment of BS-ZnO NPs, compared to cyclophosphamide (0.7-fold). Conversely, the pro-apoptotic gene Bax was markedly upregulated following treatment with BS-ZnO NPs (4.2-fold), which was comparable to the increase observed with cyclophosphamide (4.5-fold). Similarly, the tumor suppressor gene p53 showed notable upregulation, with BS-ZnO NPs inducing a 3.8-fold increase compared to cyclophosphamide, which showed a 3.5-fold increase. These findings suggest that BS-ZnO NPs effectively modulate apoptotic pathways in KB cells by decreasing Bcl-2 expression and enhancing Bax and p53 expression.

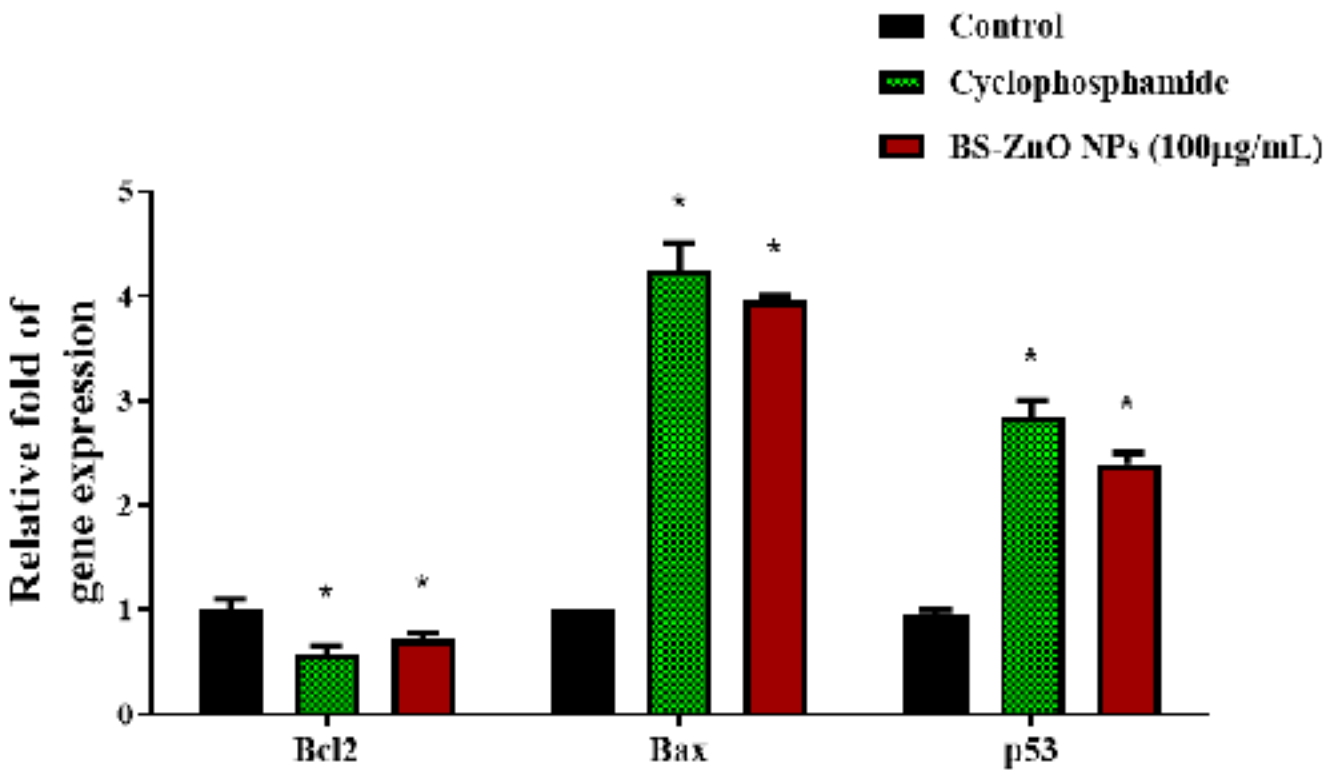

Figure 10: Gene expression was analyzed using quantitative PCR to assess the effects of BS-ZnO NPs on Bcl-2, Bax, and p53 in KB cells.

4. Discussion

The effective production and characterization of these BS-ZnO NPs in this study demonstrated their multifunctional roles in oral health, particularly in treating common oral illnesses, controlling oxidative stress, and presenting new treatment alternatives for oral cancer. One of the major factors contributing to various oral diseases is the imbalance between ROS production and the body's antioxidant defense mechanisms. The antioxidant properties of BS-ZnO NPs, demonstrated by the free radical scavenging assays, are of particular interest in the context of oral health. Similarly, the recent studies have also showed that ZnO NPs synthesized with *Ailanthus altissima* leaf extract effectively scavenged the DPPH radicals (Shabbir Awan et al., 2023). The use of BS-ZnO NPs as an antioxidant agent could, therefore, be integrated into oral care products, such as mouthwashes, toothpaste, or gels, helping to prevent oxidative damage to oral tissues, reduce gum inflammation, and protect against enamel erosion.In the oral cavity, microbial infections are the leading cause of dental diseases. *S. mutans*, for example, is a major contributor to dental caries (Al-Ansari et al., 2021), while *C. albicans* is associated with oral candidiasis (Hato et al., 2022). In this study, the antimicrobial efficacy of BS-ZnO NPs was reported to show wide range of activity against oral pathogens. The incorporation of BS into ZnO NPs could enhance this mechanism by adding another layer of action, such as inhibiting microbial enzymes. Additionally, BS itself has shown antimicrobial properties in previous studies (Pierre Luhata and Usuki, 2021), which may further contribute to the enhanced activity of BS-ZnO NPs. The results indicating BS binding interactions with key virulence proteins of oral pathogens provide a promising basis for developing targeted oral applications. For *S. aureus*, BS interaction with phospholipase C, a critical enzyme responsible for hydrolyzing host cell membrane phospholipids and promoting bacterial invasion (Nakamura et al., 2020), suggests that an inhibition-based approach could be highly effective. For *S. mutans,* BS binding with glucosyltransferase B, an enzyme crucial for synthesizing insoluble glucans and promoting biofilm formation (Zhang et al., 2021), indicates its potential to disrupt plaque development. Similarly, targeting the enterococcal surface protein in *E faecalis*, a factor contributing to adhesion and persistence in dental root canals (Gaeta et al., 2023), disrupting bacterial colonization and aiding in endodontic treatments. Lastly, the interaction of BS with adhesin Als3, a surface protein of *C. albicans* essential for fungal adhesion and invasion (Karkowska-Kuleta et al., 2021), points to its potential in managing fungal biofilms.Oral cancer, often linked to chronic dental diseases such as periodontitis and poor oral hygiene, highlights the critical interplay between persistent inflammation and carcinogenesis in the oral cavity (Komlós et al., 2021; Li et al., 2022). At the molecular level, BS-ZnO NPs show strong potential as a therapeutic option by effectively modulating apoptotic pathways. The downregulation of the anti-apoptotic gene bcl2 suggests that these NPs can interfere with cancer cell

survival mechanisms, promoting cell death. Additionally, the upregulation of the pro-apoptotic gene bax and the tumor suppressor gene p53 indicates the activation of intrinsic apoptotic pathways. This combined effect of reducing cell survival signals while enhancing cell death pathways highlights their potential to efficiently target and eliminate cancer cells.

5. Conclusion

The current study demonstrate the significant potential of BS-ZnO NPs in dental and oral health applications, particularly for managing oxidative stress, combating microbial infections, and providing novel therapeutic options for oral cancer. Future research, including in vivo studies and clinical trials, will be essential to translate these findings into practical applications, paving the way for the widespread use of BS-ZnO NPs in oral healthcare.

Declarations

Ethical Approval

This article contains no studies with human participants or animals performed by any of the authors.

Consent to Participate

Not Applicable

Consent to Publish

Not Applicable

Funding

Not Applicable

Availability of data and materials

The data that support the findings of this study are available from the corresponding author, upon reasonable request.

Author contribution

S.S and S.K contributed equally to the manuscript

Acknowledgement

Not Applicable

Conflict of Interest

The authors declare that they have no conflict of interest

Reference

1. Ahmad, Irfan, Irfan, S., Abohashrh, M., Wahab, S., Abullais, S.S., Javali, M.A., Nisar, N., Alam, M.M., Srivastava, S., Saleem, M., Zaman, G.S., Ahmad, Irshad, Mansuri, N., 2021. Inhibitory Effect of Nepeta deflersiana on Climax Bacterial Community Isolated from the Oral Plaque of Patients with Periodontal Disease. Molecules 26, 202. https://doi.org/10.3390/molecules26010202
2. Al-Ansari, M.M., Al-Dahmash, N.D., Ranjitsingh, A.J.A., 2021. Synthesis of silver nanoparticles using gum Arabic: Evaluation of its inhibitory action on Streptococcus mutans causing dental caries and endocarditis. J. Infect. Public Health 14, 324–330. https://doi.org/10.1016/j.jiph.2020.12.016
3. Alam, F., Khan, S.H.A., Asad, M.H.H. Bin, 2021. Phytochemical, antimicrobial, antioxidant and enzyme inhibitory potential of medicinal plant Dryopteris ramosa (Hope) C. Chr. BMC Complement. Med. Ther. 21, 197. https://doi.org/10.1186/s12906-021-03370-7
4. Amaya Arbeláez, M.I., de Paula e Silva, A.C.A., Navegante, G., Valente, V., Barbugli, P.A., Vergani, C.E., 2021. Proto-Oncogenes and Cell Cycle Gene Expression in Normal and Neoplastic Oral Epithelial Cells Stimulated With Soluble Factors From Single and Dual Biofilms of Candida albicans and Staphylococcus aureus. Front. Cell. Infect. Microbiol. 11. https://doi.org/10.3389/fcimb.2021.627043
5. Gaeta, C., Marruganti, C., Ali, I.A.A., Fabbro, A., Pinzauti, D., Santoro, F., Neelakantan, P., Pozzi, G., Grandini, S., 2023. The presence of Enterococcus faecalis in saliva as a risk factor for endodontic infection. Front. Cell. Infect. Microbiol. 13. https://doi.org/10.3389/fcimb.2023.1061645
6. Hato, H., Sakata, K., Sato, J., Hasebe, A., Yamazaki, Y., Kitagawa, Y., 2022. Factor associated with oral candidiasis caused by co-infection of Candida albicans and Candida glabrata: A retrospective study. J. Dent. Sci. 17, 1458–1461. https://doi.org/10.1016/j.jds.2021.10.020
7. Heidari, M., Doosti, A., 2023. Staphylococcus aureus enterotoxin type B (SEB) and alpha-toxin induced apoptosis in KB cell line. J. Med. Microbiol. Infect. Dis. 11, 96–102. https://doi.org/10.52547/JoMMID.11.2.96
8. Hong, J.M., Kim, J.E., Min, S.K., Kim, K.H., Han, S.J., Yim, J.H., Park, H., Kim, J.H., Kim, I.C., 2021. Anti-Inflammatory Effects of Antarctic Lichen Umbilicaria antarctica Methanol Extract in Lipopolysaccharide-Stimulated RAW 264.7 Macrophage Cells and Zebrafish Model. Biomed Res. Int. 2021, 1–12. https://doi.org/10.1155/2021/8812090
9. Hussain, S.A., Ramasamy, M., Shaik, M.R., Shaik, B., Deepak, P., Thiyagarajulu, N., Matharasi Antonyraj, A.P., Guru, A., 2024. Inhibition of Oral Biofilms and Enhancement of Anticancer Activity on Oral Squamous Carcinoma Cells Using Caffeine-Coated Titanium Oxide Nanoparticles. Chem. Biodivers. https://doi.org/10.1002/cbdv.202402476
10. Junge, T., Topoll, H., Eickholz, P., Petsos, H., 2021. Retrospective long-term analysis of tooth loss over 20 years in a specialist practice setting: Periodontally healthy/gingivitis and compromised patients. J. Clin. Periodontol. 48, 1356–1366. https://doi.org/10.1111/jcpe.13520
11. Kandaswamy, K., Panda, S.P., Subramanian, R., Khan, H., Shaik, M.R., Hussain, S.A., Guru, A., Arockiaraj, J.,

2024. Synergistic berberine chloride and Curcumin-Loaded nanofiber therapies against Methicillin-Resistant Staphylococcus aureus Infection: Augmented immune and inflammatory responses in zebrafish wound healing. Int. Immunopharmacol. 140, 112856.

12. Karkowska-Kuleta, J., Wronowska, E., Satala, D., Zawrotniak, M., Bras, G., Kozik, A., Nobbs, A.H., Rapala-Kozik, M., 2021. Als3-mediated attachment of enolase on the surface of Candida albicans cells regulates their interactions with host proteins. Cell. Microbiol. 23. https://doi.org/10.1111/cmi.13297
13. Khan, Z., Nath, N., Rauf, A., Emran, T. Bin, Mitra, S., Islam, F., Chandran, D., Barua, J., Khandaker, M.U., Idris, A.M., Wilairatana, P., Thiruvengadam, M., 2022. Multifunctional roles and pharmacological potential of β-sitosterol: Emerging evidence toward clinical applications. Chem. Biol. Interact. 365, 110117. https://doi.org/10.1016/j.cbi.2022.110117
14. Komlós, G., Csurgay, K., Horváth, F., Pelyhe, L., Németh, Z., 2021. Periodontitis as a risk for oral cancer: a case–control study. BMC Oral Health 21, 640. https://doi.org/10.1186/s12903-021-01998-y
15. Li, T.-J., Hao, Y., Tang, Y., Liang, X., 2022. Periodontal Pathogens: A Crucial Link Between Periodontal Diseases and Oral Cancer. Front. Microbiol. 13. https://doi.org/10.3389/fmicb.2022.919633
16. Livak, K.J., Schmittgen, T.D., 2001. Analysis of relative gene expression data using real-time quantitative PCR and the 2-ΔΔCT method. Methods 25, 402–408. https://doi.org/10.1006/meth.2001.1262
17. Marunganathan, V., Kumar, M.S.K., Kari, Z.A., Giri, J., Shaik, M.R., Shaik, B., Guru, A., 2024. Marine-derived κ-carrageenan-coated zinc oxide nanoparticles for targeted drug delivery and apoptosis induction in oral cancer. Mol. Biol. Rep. 51, 89. https://doi.org/10.1007/s11033-023-09146-1
18. Nakamura, Y., Kanemaru, K., Shoji, M., Totoki, K., Nakamura, K., Nakaminami, H., Nakase, K., Noguchi, N., Fukami, K., 2020. Phosphatidylinositol-specific phospholipase C enhances epidermal penetration by Staphylococcus aureus. Sci. Rep. 10, 17845. https://doi.org/10.1038/s41598-020-74692-8
19. Pierre Luhata, L., Usuki, T., 2021. Antibacterial activity of β-sitosterol isolated from the leaves of Odontonema strictum (Acanthaceae). Bioorg. Med. Chem. Lett. 48, 128248. https://doi.org/10.1016/j.bmcl.2021.128248
20. Rafe Hatshan, M., Perianaika Matharasi Antonyraj, A., Marunganathan, V., Rafi Shaik, M., Deepak, P., Thiyagarajulu, N., Manivannan, C., Jain, D., Melo Coutinho, H.D., Guru, A., Arockiaraj, J., 2024. Synergistic Action of Vanillic Acid-Coated Titanium Oxide Nanoparticles: Targeting Biofilm Formation Receptors of Dental Pathogens and Modulating Apoptosis Genes for Enhanced Oral Anticancer Activity. Chem. Biodivers. https://doi.org/10.1002/cbdv.202402080
21. Ravikumar, O. V., Marunganathan, V., Kumar, M.S.K., Mohan, M., Shaik, M.R., Shaik, B., Guru, A., Mat, K., 2024. Zinc oxide nanoparticles functionalized with cinnamic acid for targeting dental pathogens receptor and modulating apoptotic genes in human oral epidermal carcinoma KB cells. Mol. Biol. Rep. 51, 352. https://doi.org/10.1007/s11033-024-09289-9
22. Roberts, W.E., Mangum, J.E., Schneider, P.M., 2022. Pathophysiology of Demineralization, Part II: Enamel White Spots, Cavitated Caries, and Bone Infection. Curr. Osteoporos. Rep. 20, 106–119. https://doi.org/10.1007/s11914-022-00723-0
23. Shabbir Awan, S., Taj Khan, R., Mehmood, A., Hafeez, M., Rizwan Abass, S., Nazir, M., Raffi, M., 2023. Ailanthus altissima leaf extract mediated green production of zinc oxide (ZnO) nanoparticles for antibacterial and antioxidant activity. Saudi J. Biol. Sci. 30, 103487. https://doi.org/10.1016/j.sjbs.2022.103487
24. Shaik, M.R., Kandaswamy, K., Guru, A., Khan, H., Giri, J., Mallik, S., Shah, M.A., Arockiaraj, J., 2024. Piperine-coated zinc oxide nanoparticles target biofilms and induce oral cancer apoptosis via BCl-2/BAX/P53 pathway. BMC Oral Health 24, 715. https://doi.org/10.1186/s12903-024-04399-z
25. Tayyeb, J.Z., Guru, A., Kandaswamy, K., Jain, D., Manivannan, C., Mat, K.B., Shah, M.A., Arockiaraj, J., 2024a. Synergistic effect of zinc oxide-cinnamic acid nanoparticles for wound healing management: in vitro and zebrafish model studies. BMC Biotechnol. 24, 78. https://doi.org/10.1186/s12896-024-00906-w
26. Tayyeb, J.Z., Priya, M., Guru, A., Kishore Kumar, M.S., Giri, J., Garg, A., Agrawal, R., Mat, K.B., Arockiaraj, J., 2024b. Multifunctional curcumin mediated zinc oxide nanoparticle enhancing biofilm inhibition and targeting apoptotic specific pathway in oral squamous carcinoma cells. Mol. Biol. Rep. 51, 423. https://doi.org/10.1007/s11033-024-09407-7
27. Zhang, Q., Ma, Q., Wang, Y., Wu, H., Zou, J., 2021. Molecular mechanisms of inhibiting glucosyltransferases for biofilm formation in Streptococcus mutans. Int. J. Oral Sci. 13, 30. https://doi.org/10.1038/s41368-021-00137-1